Materials Research Proceedings 31 (2023) 448-455 https://doi.org/10.21741/9781644902592-46

Modelling the effect of tool material on material removal rate in electric discharge machining

Umair Arif[1,a*], Imtiaz Ali Khan[2,b], Faisal Hasan[2,c]

[1]Research Scholar, Department of Mechanical Engineering, Z.H. College of Engineering & Technology, Aligarh Muslim University

[2]Professor, Department of Mechanical Engineering, Z.H. College of Engineering & Technology, Aligarh Muslim University

[a]umairarif@zhcet.ac.in, [b]iakhan.me@amu.ac.in, [c]Faisalhasan@zhcet.ac.in

Keywords: Thermal Model, Electric Discharge Machining, Tool Material, Gaussian Heat Flux

Abstract. Present study aims at modelling the impact of tool materials such as copper, tungsten carbide and brass tool on the electric discharge machining of AISI 202 stainless steel. It is well known that the electrical conductivity of tool material has an influence on the current density passed through interelectrode gap and hence sparking process and MRR are affected accordingly. A finite element model was made using gaussian heat flux equation, spark radius and fraction of heat transferred to workpiece as a function of pulse on time and pulse current, latent heat in specific heat values and thermal conductivity properties. However, for the above reasons, current density used in gaussian heat flux equation was modified and electrical resistivity (which is inverse of electrical conductivity) of tool and workpiece were incorporated in it. This theorized heat flux formulae were then tested with the literature and found to give MRR similar to the literature.

Nomenclature

EDM	Electric discharge machining	Kt	Thermal conductivity
MRR	Material Removal Rate	ρ	Density
TWR	Tool Wear Rate	r_p	Spark radius
SR	Surface Roughness	R	Radius under consideration for heat flux
F_c	Energy distribution factor or fraction of heat transferred to workpiece	Qw	Heat flux applied
V	Voltage	delta T	Melting point temperature of work material - room temperature
I	Pulse current	ϱ_t	Electrical resistivity of tool
T_{on}	Pulse on time	R_t	Resistance of tool
T	Temperature	R_w	Resistance of workpiece
ϱ_W	Electrical resistivity of workpiece		

Introduction

Electric discharge machining (EDM) is an unconventional machining process where 2000-500,000 sparks/minute are generated during pulse on time. These sparks ionize the dielectric fluid at a point and impinges the workpiece resulting in an intense localized heat generation. This causes vaporization of workpiece followed by crater formation. The MRR depends on the electrical conductivity of the tool material that allows certain current density. The tool with high electrical conductivity facilitates the sparking process and increases effective discharge energy which increase MRR. [1] [2][3].

Researchers have modeled EDM process by used gaussian heat flux and spark radius as a function of process parameters [4]–[12]. Kalajahi et al. [6] and Tang et al. [9] have used spark radius as a function of pulse on time and pulse current. Joshi et al. [12] used F_c as 18.3%, PFE as

100% and spark radius as a function of pulse on time and pulse current in their 2D FEM model of a single-spark EDM process using AISI W1 tool steel workpiece. They compared their results from Dibitonto et al [13] and discovered that theirs result, better matched the experimental reading in terms of the shape of crater cavity, MRR and TWR. Further Shabgard et al.[14] used gaussian heat flux, current, and pulse on time based spark radius to develop a model that demonstrated that F_c is a function of pulse on time and current. Harminder singh also showed similar results [15]. Ming et al [16] used Harminder data in their model to develop a relationship between F_c and pulse current, pulse on time. They used that F_c in their model along with gaussian heat distribution, spark radius as a function of pulse current and pulse on time, the latent heat, and PFE and compared their results with Dibitonto et al [13] and Joshi et al.[12]. They found that their results were more comparable to experimental results. Ahmed et al [17] presented a thermal model of EDM using F_c and spark radius as a function of current, temperature dependent thermal properties of the material, latent heat of fusion and found better accuracy of the obtained results for inconel 718. M. Kliuev, et al.[18] also concluded in their model that F_c is strongly influenced by discharge current and then by pulse on time. However, authors did not find any literature that incorporates the effect of using different tool material on performance parameters in their model. Experimentally it was observed that the tools with better electrical conductivity had a major impact on discharge channel and discharge energy to workpiece resulting in better MRR[1] [2]. Hence this study models the effect of using different tool material on MRR by incorporating electrical resistivity in the heat flux formulae.

Thermal analysis model

Here, Fourier heat conduction equation is taken as governing equations, with necessary boundary conditions. Assuming that all the sparks have the same nature, a transient nonlinear analysis of single discharge EDM is performed on A1S1 202 steel. The model is then extended to all the sparks occurring during the process. During the analysis, the following presumptions were made:

1) The material of the workpiece was assumed to be isotropic and homogeneous.
2) The work domain is axis symmetric about X and Y axis.
3) Heat is transferred to the workpiece via conduction and radiation; convective heat losses are negligible.
4) Gaussian heat flux is utilized as the heat source, and only a portion of the spark energy is lost as heat in the workpiece.
5) It is assumed that the spark radius is a function of pulse current and pulse on time.
6) The fraction of heat transferred to workpiece is taken as a function of pulse on time and pulse current.

Governing equation

The Fourier heat conduction equation is used as the governing equation for the thermal analysis of the EDM process.

$$\frac{\partial T}{\alpha \partial t} = \frac{\partial T}{r \partial r} + \frac{\partial \partial T}{\partial Z^2} + \frac{\partial \partial T}{\partial r^2} \qquad 1$$

Where $\alpha = \frac{\mathrm{Kt}}{\rho(\mathrm{Cpeff}+\frac{\mathrm{m}}{\mathrm{Tm}})}$, r and z are coordinates.

Boundary conditions

Figure 1 depicts the model's assumed boundary conditions. A Gaussian heat flux distribution represents the heat transferred to the workpiece during the pulse on-time on the top surface. Surface B1 shows convective heat transfer to the dielectric for $R \geq r_p$. Surfaces B2, B3, and B4 are considered as insulated and no heat transfer occur across them. The initial temperature is considered equal to dielectric temperature. The applied boundary and initial conditions are represented mathematically as

$$k\frac{\partial T}{\partial Z} = Qw \text{ for } R \le r_p \text{ on B1} \qquad 2$$

$$\frac{k\,\partial T}{\partial Z} = hc\,(T - To) \text{ for } R \ge r_p \text{ on B1}$$

$$\frac{k\partial T}{\partial Z} = 0 \text{ for } T_{off} \text{ (Pulse off time)}$$

$$\frac{\partial T}{\partial Z} = 0 \text{ for B2, B3, B4.}$$

Where h_c is the dielectric fluid's heat transfer coefficient and T_0 (K) is the initial temperature of dielectric before starting of the EDM process.

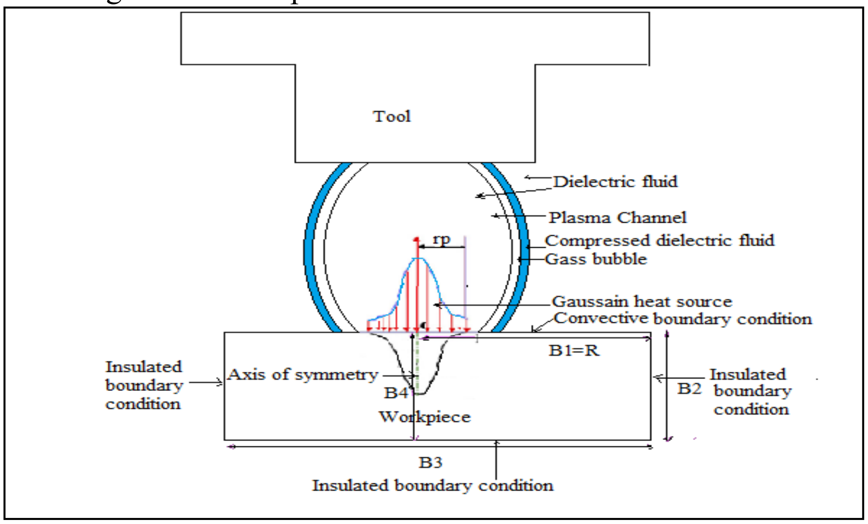

Figure 1 Axis symmetric model as well as boundary conditions

Heat flux

Many researchers have demonstrated that the gaussian heat flux distribution is more realistic and produces better results [12] [16]. Patel at el. [19] proposed a Gaussian-based heat input formulation for thermal modelling of the EDM process, which has been used by many researchers [12], [20].

$$Q = 4.57\frac{FcVI}{\pi rp^2}EXP\{-4.5\left(\frac{R}{rp}\right)^2$$

3

Total resistance offered to flow of current in EDM can be written= $R_t + R_w$

$$Resistance = \frac{\rho * length}{Area} \qquad 4$$

The fraction of the total current that flows through the tool is given by:

$$\frac{Current\ tool}{Current\ total} = \frac{Rt}{(Rt + Rw)} = \frac{\rho t}{\rho t + \rho w} \qquad 5$$

To incorporate the effect of tool material on heat flux we replaced the energy density $(\frac{VI}{\pi rp^2})$ in the equation 3 by $(\frac{VI\left(\frac{\rho t}{\rho t+\rho w}\right)}{\pi rp^2})$. However still the simulation reading was not the same as in the experiment[1], so by using the initially obtained simulation readings and comparing it with experiment readings in literature[1], the exponential power was calculated. The final heat flux equation became as shown in equation 6. This heat flux was then validated by using the experimental reading in the literature[1].

Materials Research Proceedings 31 (2023) 448-455 https://doi.org/10.21741/9781644902592-46

$$Q = 4.57 \frac{FcVI\left(\frac{ft}{ft+fw}\right)^{0.299}}{\pi rp^2} EXP\{-4.5\left(\frac{R}{rp}\right)^2$$

6

Spark radius is an important parameter to consider when modelling the EDM process. In the literature, various researchers have proposed spark radius as a point source, constant radius, or as a function of pulse current and pulse on time. However, Ikai and Hashiguchi's [21] showed that EDM radius calculations are more accurate when based on a semiempirical equation in equation 7.

$$rp = (2.04e - 3)I^{0.43}\, Ton^{0.44} \quad 7$$

Energy distribution factor

Another important factor in modelling EDM process is the energy distribution factor or fraction of heat transferred to workpiece (F_c). Shabgard et al.[14] demonstrated that the fraction of heat absorbed by the electrodes varied with pulse current (I) and Pulse on time (T_{on}). Shabgard defined F_c as $F_c = 5.5998xI^{-0.3401}xT_{on}^{0.2989.}$ As a result, it was decided to model the results by using F_c as the function provided by Shabgard et al.[14].

Plasma flushing efficiency

Plasma flushing efficiency is the ratio of the actual volume of material eliminated per pulse to the theoretical volume of material melted per pulse. It is determined as

$$PFE = \frac{Volume\ Exp}{Volume\ FEM} * 100 \quad 8$$

Table 1 Mechanical properties of AISI 202 stainless steel and tools used

AISI 202 stainless steel								
Electrical resistivity (ohm-cm)	Tensile yield strength (MPa)	Specific heat capacity (C_p)(J/kg^{o}c)	Melting point (^{o}C)	Density (kg/m^3)	Young 'modulus (Gpa)	Poisson's ratio	Thermal conductivity (W/m-k)	Thermal expansion coefficient (1/^{o}c)
6.9E-7	275	500	1450	7800	200	0.28	16.2	2.06x10^{-5}

Copper tool	Brass tool	Tungsten tool
Electrical resistivity – 1.67E-8	Electrical resistivity - 5.98E-7	Electrical resistivity – 1.56E--7

Results

Table 2 shows simulated MRR and SR readings for different tool material at 9A current and 0.4 duty cycle.

Tool material	Current 9 A				
	Gap voltage	spark radius	Radius (mm)	Height (mm)	MRR (mm^3/min)
Not considering any tool material	40	6.09E-05	0.037	0.017	23.46585
Copper tool	40	6.09E-05	0.018	0.005	1.56529
Brass tool	40	6.09E-05	0.026	0.009	5.960034
Tungsten carbide tool	40	6.09E-05	0.03	0.012	10.71619

Copper tool	60	6.09E-05	0.026	0.01	6.68192
Brass tool	60	6.09E-05	0.032	0.013	13.22976
Tungsten carbide tool	60	6.09E-05	0.036	0.015	19.37223
Copper tool	80	6.09E-05	0.03	0.012	10.71619
Brass tool	80	6.09E-05	0.035	0.015	18.369
Tungsten carbide tool	80	6.09E-05	0.039	0.018	27.62132

*Fraction of heat transferred to the workpiece was calculated as 7.989 % using Shabgard et al.[14] equation, Pulse on time was taken as 40µs and Pulse off time was taken as 60µ.

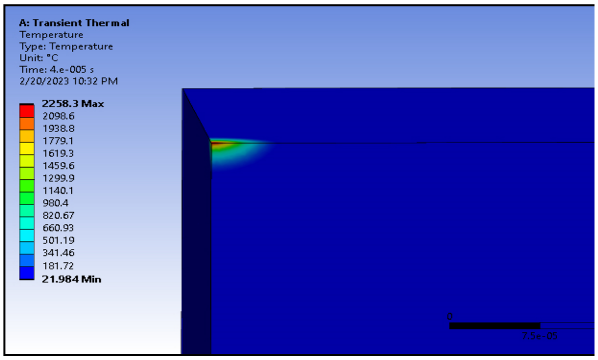

Figure 2 shows the simulation of AISI 202 Stainless steel using Copper tool at 9A.

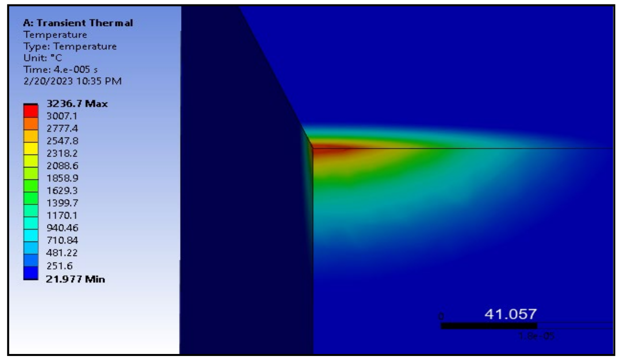

Figure 3 shows the simulation of AISI 202 Stainless steel using Brass tool at 9A.

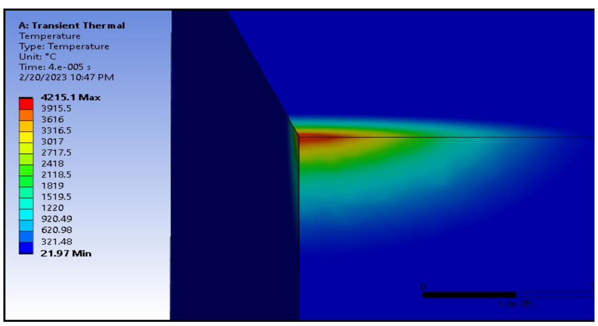

Figure 4 shows the simulation of AISI 202 Stainless steel using Tungsten carbide tool at 9A.

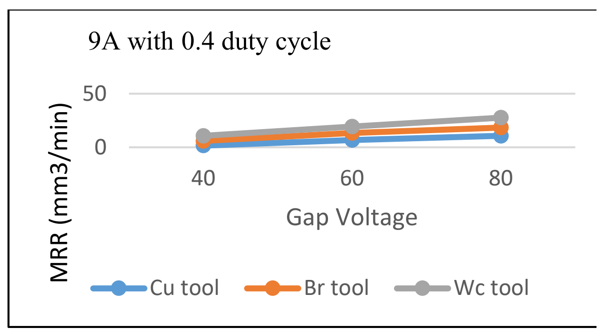

Figure 5 shows the predicted MRR results from the model for different tool materials at 9A.

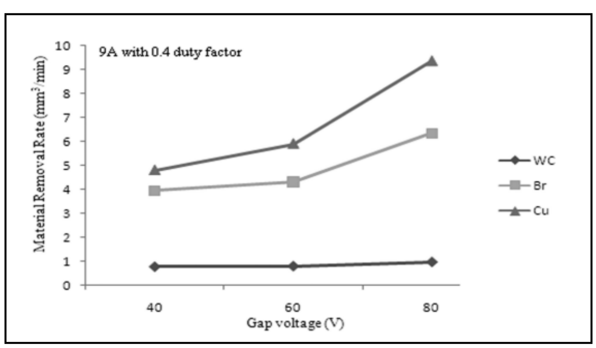

Figure 6 show the MRR results of Muthuramalingam and Mohan[1] at 9A.

Discussion

In this research, a thermal model was developed for the EDM process using a Gaussian heat flux, spark radius, and F_c, as functions of pulse on time and pulse current, specific heat values and thermal conductivity properties. The Finite Element Modelling method was used to solve the differential equation with the above-described boundary conditions using Ansys transient thermal. The axisymmetric workpiece model was used. The material properties from Table 1 were given to Ansys. At the spark position, the mesh size was refined for improved convergence of results. The gaussian heat fluxes was calculated incorporating the F_c values calculated using Shabgard et al.[14] equation. The gap voltage was taken as 40, 60, 80 V. The spark radius obtained from the above equation was divided into ten parts and accordingly the Gaussian heat flux was calculated and applied to each part. On the remaining area, convective boundary conditions were used to generate temperature profiles. The convective heat transfer coefficient was taken into account to be 10,000 W/m^2K.The melting temperature of AISI 202 stainless steel ie 1450ºC was chosen as the temperature for crater formation, as shown in Figure *2*. Nodes with temperatures higher than the melting point of AISI 202 stainless steel were eliminated.

It is experimentally proven that tool material with better electrical conductivity gave more MRR[1] [2]. Using this fact, the same has been incorporated in the gaussian heat flux formulae. As a consequence, the energy density in gaussian heat flux ie VI/ πr^2 was modified as $\left(\frac{VI\left(\frac{\mathcal{f}t}{\mathcal{f}t+\mathcal{f}w}\right)}{\pi rp^2}\right)$. However, modifying the current by multiplying it by simple ratio $\left(\frac{\mathcal{f}t}{\mathcal{f}t+\mathcal{f}w}\right)$did not gave good results for all materials. MRR reading was obtained from the model and compared to the obtained from literature[1]. It was observed that the model reading was much larger than the experimental values[1]. Hence by comparing the simulation reading and the experimental reading[1], the exponential power was calculated and the ratio become $\left(\frac{\mathcal{f}t}{\mathcal{f}t+\mathcal{f}w}\right)^{0.299}$ which gave much closer results to experimental values.

The resulting isotherms obtained from Ansys are shown in Figure *2* to Figure 4. Table 2 shows the coordinates of the crater formed. Crater volume is determined by using formulae in equation 9. MRR is calculated by multiplying the crater volume by the number of pulses per minute as shown in equation 10 and 11 [22]. Table 2 displays the final results.

$$\text{Crater volume} = 3.14 * \text{height of crater} * \frac{3*(\text{radius of crater})^2+(\text{height of crater})^2}{6} \tag{9}$$

$$\text{Total no of pulses per min} = \frac{60}{\text{pulse on time+pulse off time}} \tag{10}$$

$$\text{MRR} = \text{Crater volume} * \text{Number of pulses per min} \tag{11}$$

The proposed finite element model gave MRR readings for three tool materials namely copper, brass and tungsten carbide by incorporating their electrical resistivity in the gaussian heat flux formulae. These readings were validated from literature [1] and graphs were plotted as depicted in Figure 5. It was observed that the modified heat flux formula readings as shown in Figure 5, gave similar trends for all three tool materials as obtained in literature [1] also depicted in Figure 6. Hence this model shows better agreement with the experimental reading for different tool materials. It was observed from the model results that for all three tools, tool material having larger electrical conductivity gave more the MRR for same process parameters. Besides it was also observed that increasing the gap voltage results in improved MRR for same current values.
However, predicted values differed from the literature values which can be explained by the fact that the simulation was modelled for a single spark as well as plasma flushing efficiency was not incorporated in the model. This also means that above gaussian heat source model has a potential to be further developed by incorporating a better regression analysis and validating it with more experiments.

Conclusion

The present study aims to investigate the impact of tool materials, such as, tungsten carbide, copper and brass on electric discharge machining of AISI 202 stainless steel. It is well known that the electrical conductivity of the tool material plays a crucial role in determining the current density passing through the interelectrode gap, thereby affecting the discharging process and MRR. To develop a finite element model of EDM, a Gaussian heat flux equation was employed, which incorporated spark radius, fraction of heat transferred to the workpiece as a function of pulse current and pulse on time, specific heat values, and thermal conductivity properties. However, to account for the effect of electrical conductivity, modifications were made to the energy density used in the heat flux equation, and the electrical resistivity of both the tool and workpiece was incorporated. The proposed heat flux equation was validated against existing literature, and the results showed that the MRR obtained was in good agreement. Besides it was observed that increasing tool materials electrical conductivity or gap voltages resulted in improved MRR. However, the predicted values obtained from the simulation were found to be higher than the experimental values. This discrepancy can be explained by the fact that the simulation model was designed for a single spark and did not take into account the plasma flushing efficiency. Such improvements would enhance the accuracy and applicability of the model.

Reference

[1] T. Muthuramalingam and B. Mohan, “Influence of tool electrode properties on machinability in spark erosion machining,” *Mater. Manuf. Process.*, vol. 28, no. 8, pp. 939–943, 2013. http://doi.org/10.1080/10426914.2013.763973

[2] M. P. Jahan, Y. S. Wong, and M. Rahman, “A study on the fine-finish die-sinking micro-EDM of tungsten carbide using different electrode materials,” vol. 9, pp. 3956–3967, 2008. http://doi.org/10.1016/j.jmatprotec.2008.09.015

[3] U. Arif, I. Ali Khan, and F. Hassan, “Green and sustainable electric discharge machining: a review,” *Adv. Mater. Process. Technol.*, vol. 00, no. 00, pp. 1–75, 2022. http://doi.org/10.1080/2374068X.2022.2108599

[4] V. Yadav, V. K. Jain, and P. M. Dixit, “Thermal stresses due to electrical discharge machining,” *Int. J. Mach. Tools Manuf.*, vol. 42, no. 8, pp. 877–888, 2002. http://doi.org/10.1016/S0890-6955(02)00029-9

[5] S. H. Yeo, W. Kurnia, and P. C. Tan, “Electro-thermal modelling of anode and cathode in micro-EDM,” *J. Phys. D. Appl. Phys.*, vol. 40, no. 8, pp. 2513–2521, 2007. http://doi.org/10.1088/0022-3727/40/8/015

[6] M. Hosseini Kalajahi, S. Rash Ahmadi, and S. Nadimi Bavil Oliaei, “Experimental and finite element analysis of EDM process and investigation of material removal rate by response surface methodology,” *Int. J. Adv. Manuf. Technol.*, vol. 69, no. 1–4, pp. 687–704, 2013. http://doi.org/10.1007/s00170-013-5059-x

[7] S. Plaza, I. Pombo, N. Ortega, B. Ã. Izquierdo, and J. A. Sa, “International Journal of Machine Tools & Manufacture A numerical model of the EDM process considering the effect of multiple discharges,” vol. 49, pp. 220–229, 2009. http://doi.org/10.1016/j.ijmachtools.2008.11.003

[8] H. K. Kansal, S. Singh, and P. Kumar, “Numerical simulation of powder mixed electric discharge machining (PMEDM) using finite element method,” *Math. Comput. Model.*, vol. 47, no. 11–12, pp. 1217–1237, 2008. http://doi.org/10.1016/j.mcm.2007.05.016

[9] L. Tang, L. Ren, and Q. L. Zhu, "EDM multi-pulse temperature field simulation of SiC/Al functionally graded materials," *Int. J. Adv. Manuf. Technol.*, vol. 97, no. 5–8, pp. 2501–2508, 2018. http://doi.org/10.1007/s00170-018-2136-1

[10] M. Singh, P. Saxena, J. Ramkumar, and R. V. Rao, "Multi-spark numerical simulation of the micro-EDM process: an extension of a single-spark numerical study," *Int. J. Adv. Manuf. Technol.*, vol. 108, no. 9–10, pp. 2701–2715, 2020. http://doi.org/10.1007/s00170-020-05566-6

[11] K. P. Somashekhar, S. Panda, J. Mathew, and N. Ramachandran, "Numerical simulation of micro-EDM model with multi-spark," *Int. J. Adv. Manuf. Technol.*, vol. 76, no. 1–4, pp. 83–90, 2015. http://doi.org/10.1007/s00170-013-5319-9

[12] S. N. Joshi and S. S. Pande, "Development of an intelligent process model for EDM," *Int. J. Adv. Manuf. Technol.*, vol. 45, no. 3–4, pp. 300–317, 2009. http://doi.org/10.1007/s00170-009-1972-4

[13] D. D. Dibitonto, P. T. Eubank, M. R. Patel, M. A. Barrufet, and D. D. Diitonto, "Theoretical models of the electrical discharge machining process . I . A simple cathode erosion model Theoretical models of the electrical discharge machining process . I . A simple cathode erosion model," vol. 4095, no. 1989, 1989. http://doi.org/10.1063/1.343994.

[14] M. Shabgard, R. Ahmadi, M. Seyedzavvar, and S. N. B. Oliaei, "Mathematical and numerical modeling of the effect of input-parameters on the flushing efficiency of plasma channel in EDM process," *Int. J. Mach. Tools Manuf.*, vol. 65, pp. 79–87, 2013. http://doi.org/10.1016/j.ijmachtools.2012.10.004

[15] H. Singh, "Experimental study of distribution of energy during EDM process for utilization in thermal models," *Int. J. Heat Mass Transf.*, vol. 55, no. 19–20, pp. 5053–5064, 2012. http://doi.org/10.1016/j.ijheatmasstransfer.2012.05.004

[16] W. Ming *et al.*, "A hybrid process model for EDM based on finite-element method and Gaussian process regression," *Int. J. Adv. Manuf. Technol.*, vol. 74, no. 9–12, pp. 1197–1211, 2014. http://doi.org/10.1007/s00170-014-5989-y

[17] A. Ahmed, A. Fardin, M. Tanjilul, Y. S. Wong, M. Rahman, and A. Senthil Kumar, "A comparative study on the modelling of EDM and hybrid electrical discharge and arc machining considering latent heat and temperature-dependent properties of Inconel 718," *Int. J. Adv. Manuf. Technol.*, vol. 94, no. 5–8, pp. 2729–2737, 2018. http://doi.org/10.1007/s00170-017-1100-9

[18] M. Kliuev, K. Florio, M. Akbari, and K. Wegener, "In fl uence of energy fraction in EDM drilling of Inconel 718 by statistical analysis and fi nite element crater-modelling," *J. Manuf. Process.*, vol. 40, no. February, pp. 84–93, 2019. http://doi.org/10.1016/j.jmapro.2019.03.002

[19] M. R. Patel, M. A. Barrufet, P. T. Eubank, and D. D. Dibitonto, "Theoretical models of the electrical discharge machining process . II . The anode erosion model," vol. 4104, 1989. http://doi.org/10.1063/1.343995

[20] S. N. Joshi and S. S. Pande, "Thermo-physical modeling of die-sinking EDM process," *J. Manuf. Process.*, vol. 12, no. 1, pp. 45–56, 2010. http://doi.org/10.1016/j.jmapro.2010.02.001

[21] T. Ikai and K. Hashigushi, "Heat input for crater formation in EDM," in *In Proceedings of the International Symposium for Electro-Machining-ISEM XI, EPFL*, 1995, pp. 163–170.

[22] Vishwakarma, A. Dvivedi, and F. E. Analysis, "FINITE ELEMENT MODELING OF MATERIAL REM OVAL RATE IN POWDER MIXED ELECTRIC DISCHARGE MACHINING OF AL-SIC METAL MATRIX COMPOSITES," no. iii, pp. 151–158, 2013.

[23] M. A. Younis, M. S. Abbas, M. A. Gouda, F. H. Mahmoud, and S. A. Abd, "Effect of electrode material on electrical discharge machining of tool steel surface," pp. 977–986, 2015.